UFL/COEL/MPR-2001/003

EVALUATION OF SEDIMENT TRAP EFFICIENCY IN AN ESTUARINE ENVIRONMENT

by

DANIEL MARK STODDARD

MASTER'S PROJECT REPORT

2001

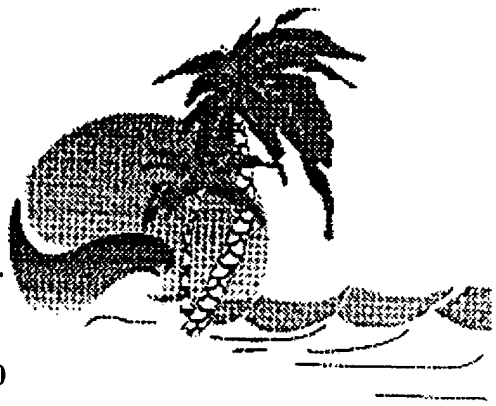

Coastal & Oceanographic Engineering Program
Department of Civil & Coastal Engineering
433 Weil Hall •P.O. Box 116590 • Gainesville, Florida 32611-6590

UNIVERSITY OF FLORIDA

EVALUATION OF SEDIMENT TRAP EFFICIENCY IN AN ESTUARINE ENVIRONMENT

By

Daniel Mark Stoddard

A REPORT PRESENTED TO THE DEPARTMENT OF CIVIL AND COASTAL
ENGINEERING OF THE UNIVERSITY OF FLORIDA
IN PARTIAL FILLFILLMENT OF THE REQUIREMENTS
FOR THE DEGREE OF MASTER OF SCIENCE

UNIVERSITY OF FLORIDA

2001

AD NUMBER	DATE	DTIC ACCESSION NOTICE
	17 JUNE 2002	

1. REPORT IDENTIFYING INFORMATION

A. ORIGINATING AGENCY

NAVAL POSTGRADUATE SCHOOL, MONTEREY, CA 93943

B. REPORT TITLE AND/OR NUMBER

EVALUATION OF SEDIMENT TRAP EFFICIENCY IN AN ESTUARINE ENVIRONMENT

C. MONITOR REPORT NUMBER

BY: DANIEL MARK STODDARD, UNIV OF FLORIDA

D. PREPARED UNDER CONTRACT NUMBER

N62271-97-G- 0052

2. DISTRIBUTION STATEMENT

APPROVED FOR PUBLIC RELEASE
DISTRIBUTION UNLIMITED

REQ

1. Put on n
2. Com
3. Attac mail
4. Use u infor
5. Do no for 6

DTIC:

1. Assign
2. Return

20020710 023

DTIC Form 50
JUL 96

PREVIOUS EDITIONS ARE OBSOLETE

ACKNOWLEDGEMENT

I would like to thank Dr. Ashish Mehta for his guidance, patience, and insight during my research and evaluation of the project tasks. Also, I would like to thank Dr. Robert Dean and Dr. Robert Thieke for being on my committee.

I would also like to thank Neil Ganju for sharing his knowledge and understanding of the modeling programs with me (as frustrating as it was for him). Additionally, without Fernando Marván and his extensive computer modeling ability, this project would not have been possible.

TABLE OF CONTENTS

LIST OF FIGURES

LIST OF TABLES

LIST OF SYMBOLS

A	area
C	sediment concentration (kg/m^3)
C_1	sediment concentration (kg/m^3) related to Equation 2.13
C_z	Chézy discharge coefficient
$D_x, D_{xx}, D_{xy}, D_{yx}, D_{yy}$	horizontal dispersion coefficients
H	depth (m)
H_e	equilibrium bed elevation related to Equation 5.1
H_0	datum bed elevation related to Equation 5.1
K	sedimentation coefficient related to Equation 5.1
K_L, K_T	longitudinal and transverse dispersion constants, respectively
L	channel length
L_o	original trap length related to Equation 4.11
M	number of time steps in one ebb tidal period
Oc	organic content (%)
P	tidal prism (m^3)
Pe	Peclet number
Q	discharge (m^3/s)
Q_d	depositional flux (kg/m^2-s)
Q_e	erosional flux (kg/m^2-s)
Q_f	freshwater discharge (m^3/s)
R	sediment removal ratio
R^2	correlation coefficient

R_{ave}	ebb-tide averaged removal ratio
S	sediment source/sink term
Sa	salinity (ppt)
S_R	sedimentation rate (m/d)
T	tidal period (s)
U	depth-averaged, x-direction velocity (m/s)
V	depth-averaged, y-direction velocity (m/s)
W_s	settling velocity (m/s)
W_{sf}	free settling velocity (m/s)
a	empirical coefficient related to Equation 2.13
b	empirical coefficient related to Equation 2.13
g	acceleration due to gravity (m/s^2)
h	water depth
Δh	deposit thickness
k	damped wave number
k_0	frictionless wave number
m	empirical coefficient related to Equation 2.13 and 4.11
n	Manning's flow resistance coefficient related to Equation 2.13
n_s	sediment bed porosity
n_w	empirical coefficient related to Equation 2.13
p	probability of deposition
q	sediment load (kg/s)
q_e	influent sediment load (kg/s)

q_i	effluent sediment load (kg/s)
t	time
Δt	time step
u_b	bottom, x-direction velocity
v_b	bottom, y-direction velocity
w_c	sediment water content
x	horizontal coordinate
y	horizontal coordinate
z	vertical coordinate
α_s	empirical coefficient related to Equation 2.16
β_s	empirical coefficient related to Equation 2.16
γ	bottom friction-dependent coefficient
ε_N	erosion rate constant (kg/m^2-s)
ε_{NO}	limiting erosion rate constant (kg-N/s)
η	water surface elevation
λ	tidal influencing factor related to Equation 4.12
ν	eddy viscosity
ρ_b	sediment bulk density (kg/m^3)
ρ_d	bottom sediment dry density (kg/m^3)
ρ_s	sediment granular density (kg/m^3)
ρ_w	water density (kg/m^3)
τ_b	bed shear stress (Pa)
τ_d	critical shear stress for deposition (Pa)

τ_s	bed shear strength (Pa)
Φ	solids volume fraction
Φ_e	limiting solids volume fraction

ABSTRACT

Abstract of Report Presented to the Graduate School
of the University of Florida in Partial Fulfillment of the
Requirements for the Degree of Master of Science

EVALUATION OF SEDIMENT TRAP EFFICIENCY IN AN ESTUARINE ENVIRONMENT

By

Daniel Mark Stoddard

December 2001

Chairman: Ashish J. Mehta
Major Department: Civil and Coastal Engineering

Trench-traps are utilized where sediment containment is a concern. In this study, trapping efficiency is key concern. A 60 m(L) x 300 m(W) x 2 m(D) trap was incorporated into the Cedar River, near the confluence with the Ortega River. A second trap of same dimensions was also incorporated 420 m upstream. Trap efficiency was calculated as a sediment removal ratio, or the percentage by which influent sediment load to the trap is reduced in the effluent load from the trap. Trap efficiency was carried out for varying Cedar River discharges. A specific discharge (16.4 m^3/s) was found to yield the maximum removal. At discharges above and below this discharge, the removal ratio decreases. This is attributed to the increase in tidal influence at lower discharges and velocities too large to allow settling at higher discharges.

Future work includes developing a monitoring scheme to determine actual sedimentation rates in a test trap at the chosen location.

CHAPTER 1
INTRODUCTION

1.1 Problem Statement

Sediment shoaling in estuarine environments can create significant problems such as decreased discharges, degradation of water quality, and concentration of contaminants and organic compounds. One commonly employed solution to reduce sedimentation is the implementation of a trap scheme by creating a trench along the submerged bottom. To create a trench-trap, the depth at the chosen location is increased by dredging. In this study, a sediment trap is defined as an area of the submerged bottom deepened to a depth greater than the surrounding bottom, in order to reduce flow velocity. The lower velocity should allow sediment to deposit in the trap rather than move past and deposit elsewhere. This in turn allows for maintenance dredging to be performed at a specific location (the trap) rather than over a broad submerged area. The increased depth results in a decreased flow velocity, thereby allowing incoming sediment to settle in the trap itself, instead of being carried further downstream. The sediment can then be removed from the trap, rather than dredging the otherwise distributed deposit from a broader area. By holding the trap depth and location constant and varying the discharge of the river system, the efficiency of a trap can be assessed for different flow discharges. For present purposes, efficiency will be determined by the sediment removal ratio, which is the percentage by which the effluent sediment load (leaving the trap) is reduced with respect to influent load entering the trap (Ganju, 2001). By creating efficient traps much of the detrimental effects of excess sediment and unwanted pollutants entering the system can be curtailed.

1.2 Role of Florida Sediment

In Florida's biologically highly active estuarine and lacustrine environments, the fraction of fine-grained sediment that is organic is often on the order of 20-60% by weight and sometimes as high as 90-95%. There are three main sources of this organic matter. Terrestrial systems tend to be abundant in carbon (C), and the biomass produced by woodland and grassland is on the order of 50g C/m^2 (Mehta et al., 1997). Much of this material is degraded by the soil but some of it is washed away and introduced into fresh water and marine environments. The composition of this material is mainly cellulose which is non-degradable by water itself and the existing soil is less efficient in degrading the organic material making its breakdown very slow. Although aquatic plants breakdown more easily, they also contribute to the input of organic matter. The third source of organic matter is provided by phytoplankton, which usually has a biomass of 1.5C/m^2 with 5-6 crops/year for the Florida region. Trefry et al. (1992) state that the coastal waterways in Florida are stressed by inputs of fine-grained organic-rich sediments from riverine systems. Besides the alterations of the benthic community that this input causes, there are indirect problems associated with organic sediment such as sorption of contaminants like Cd, Cu, Hg, Pb, Zn and PCB's. In the Cedar River, PCB's in sediment have been documented to be up to 0.023 ppm (Campbell et al., 1993) and detectable amounts (up to 0.055 ppm) are also found in every species of fish collected from the area.

Most of Florida estuaries are microtidal, hence another important feature of the region is the occurrence of episodic events such as heavy rainfall and storms which act as natural dredging mechanisms due to the strong currents generated (Marván et al., 2001).

The area of study is the Cedar River system located in Northeast Florida. Trapping contaminants in the Cedar River system is important due to the elevated concentration of PCB

(polychlorinated biphenyl) contaminants in the water system due to leeching of sediments and runoff from a fire at a chemical company in January 1984. The site was located approximately 0.35 miles east of the Cedar River near the headwaters north of Interstate I-10 and also adjacent to municipal storm drains and drainage ditches. The fire destroyed several tanks storing high concentrations (4,425 ppm) of PCB laden oils and other materials. It is believed that a combination of the damage to the storage tanks and the fire fighting effort created a vehicle for the PCB contaminant to enter the Cedar River basin. The surrounding groundwater and soil was sampled extensively in 1989 and the concentrations were still significantly above the regulated amount of 50 ppm.

The filtering role of estuaries makes them crucial transitional areas trapping significant quantities of particulate and dissolved matter through a wide variety of physical and biogeochemical processes. Cohesive sediments play an important role in these processes. Unlike sand, well characterized by its grain size distribution, cohesive sediments are complex mixtures of different clay minerals, mainly organic matter, and a small percentage of sand and silt. Hydrodynamic action is the most important mechanism involved in sediment transport. It advects the suspended sediments, provides the force needed to erode the bed and, through turbulence, plays a major role in the flocculation of cohesive sediments. Relatively large velocities generally occur in tidal estuaries. Because the hydrodynamic processes involved in sediment transport are mainly non-linear, the sediments are very mobile in these estuaries. They are eroded and transported upwards during flood, deposited during slack water, eroded again and transported downwards during ebb and redeposited during next slack water, to restart their movement in the forthcoming tidal cycle. Cohesive and non-cohesive sediments are different from each other in two major aspects: flocculation and consolidation of deposited material with

compaction of the sediments. Flocs are formed by joining individual particles and can strongly modify the settling velocity of particulate matter. After bottom deposition, the water content is still a significant part of the bed material. The expulsion of this water is part of the sediment consolidation process. The small pore dimensions imply long times for sediment deposition, which creates conditions for fluid–mud formation in environments with very high availability of sediments (Cancino and Neves, 1999).

Fine-grained cohesive sediments are important in two types of engineering problems. The first relates to the sedimentation of harbors and channels and to dredging and navigation, and the second to the mixing and dispersion of contaminants. The properties of muddy sediments are significantly affected by chemical and biological factors. As a result of their cohesive nature, mud particles absorb pollutants, especially heavy metals and pesticides. As a result, understanding pollutant dispersion depends on an understanding of particle transport. The ubiquitous bacteria and other organisms secrete films that act as a very effective glue in enhancing the resistance of the bed to erosion. However, it is noteworthy that, in general, bioturbation acts both to increase cohesiveness and also to loosen beds and resuspend sediment (Mehta and Dyer, 1990).

1.3 Objective and Tasks

The main objective is to determine how sediment traps respond to variable discharges (concentration and velocity) in the Cedar River estuarine system by analyzing the trapping efficiency.

Several tasks must be undertaken to determine the efficiency of this selected trapping scheme. These include:

1) Utilization of data collected from the field and from the existing literature to characterize the nature of the flow. This includes the tidal elevations and current velocities in the river system, and streamflow data for major tributaries from the literature.

2) Analysis of the data collected to characterize the nature of the sediment to determine the historical suspended sediment concentration data.

3) Modeling the flow field via a hydrodynamic model, in order to determine the velocities as well as the water surface elevations.

4) Reevaluation and recalculation of rating curve results from previous analysis. This new curve will be used to calculate concentrations associated with the varying discharges.

5) Utilization of a sediment transport model to determine suspended sediment concentrations. This model will incorporate the sediment characteristics determined from the sediment analysis.

6) Two trap locations will be evaluated in the calibrated flow model, and the output from that model will be applied to the calibrated sediment transport model. The influent and effluent sediment loads through the trap will be recorded in order to quantify trap efficiency of each trap.

1.4 Report Outline

The following sections of the report will describe how the trap efficiency will be evaluated and the modeling efforts required. Next, a basic description of the Cedar and Ortega River system will be provided. The report will continue with development of the sediment rating curves, the trap design selection and the efficiency analysis of the selected trap. The summary, conclusions and recommendations will complete the report followed by a bibliography.

CHAPTER 2
METHOD OF ANALYSIS

2.1 Trap Efficiency

The modeling of trap efficiency requires the use of a flow and sediment transport model. A flow model will provide water velocities and surface elevations, and these solutions will be applied to a sediment transport model. The sediment transport model will predict erosion, deposition, and suspended sediment concentrations in the presence of the trap.

2.2 Flow Modeling

2.2.1 Governing Equations

The Navier-Stokes equations govern the free surface flows of constant density and incompressible fluids (Pnueli and Gutfinger, 1992). Applying the hydrostatic pressure distribution assumption yields three-dimensional model equations, and these can be vertically integrated to produce the following two-dimensional shallow water equations (Casulli, 1990):

x-momentum:

$$\frac{\partial(HU)}{\partial t}+\frac{\partial(HUU)}{\partial x}+\frac{\partial(HUV)}{\partial y}=-gH\frac{\partial \eta}{\partial x}+\frac{\partial}{\partial x}\left(\nu H\frac{\partial U}{\partial x}\right)+\frac{\partial}{\partial y}\left(\nu H\frac{\partial U}{\partial y}\right)-\gamma U \qquad (2.1)$$

y-momentum:

$$\frac{\partial(HV)}{\partial t}+\frac{\partial(HUV)}{\partial x}+\frac{\partial(HVV)}{\partial y}=-gH\frac{\partial \eta}{\partial y}+\frac{\partial}{\partial x}\left(\nu H\frac{\partial V}{\partial x}\right)+\frac{\partial}{\partial y}\left(\nu H\frac{\partial V}{\partial y}\right)-\gamma V \qquad (2.2)$$

continuity:

$$\frac{\partial \eta}{\partial t}+\frac{\partial(HU)}{\partial x}+\frac{\partial(HV)}{\partial y}=0 \qquad (2.3)$$

where H is the water depth, U is the vertically-averaged horizontal x-direction velocity, V is the vertically-averaged horizontal y-direction velocity, t is time, g is the acceleration due to gravity,

η is the water surface elevation measured from the undisturbed water surface, ν is the eddy viscosity, and γ is the bottom friction dependent coefficient defined as

$$\gamma = \frac{g\sqrt{u_b^2 + v_b^2}}{C_z^2} \tag{2.4}$$

where u_b and v_b are the horizontal x and y bottom velocity components respectively, and C_z is the Chézy discharge coefficient, which is related to Manning's n by

$$C_z = \frac{(H+\eta)^{1/6}}{n} \tag{2.5}$$

Solving this system of three partial differential equations (Equations 2.1, 2.2, and 2.3) for the three unknowns (U, V, η) can be accomplished via a numerical method. The numerical algorithm used is based on the method developed by Casulli (1990). First, a characteristic analysis is performed on Equations 2.1-2.3, in order to determine which terms must be discretized implicitly, such as the water surface elevation (Eqs. 2.1, 2.2), and the velocity divergence (Equation 2.3). The advective terms are discretized explicitly using an upwind scheme, which is unconditionally stable when a Eulerian-Lagrangian method is used to discretize the terms. This method requires the solution of a 5-diagonal matrix at every time step. It is used in conjunction with an alternating-direction implicit (ADI) routine, which results in two simpler, linear tri-diagonal matrices (Casulli, 1990).

2.2.2 Model Operation

The 2-D vertically averaged hydrodynamic model reported by Marván (2001) which was developed by Casulli (1990) used in this study is operated using the MATLAB computational computer application. The use of MATLAB allows for the generation of the necessary graphics and data output in a simple fashion, though the computational effort is intensive, due to the necessity of large matrices. Rectangular grids with square elements are used, with numeric

"ones" indicating the body of water, and "zeros" representing land boundaries developed for input into the computer model. A similar grid is required for the input bathymetry, with the depth at mean high water entered into each element.

2.2.3 Flow Boundary Conditions

Flow boundaries are indicated by extending water cells to the grid edge. If freshwater inflow is desired, a permanent velocity can be imposed at the edge, corresponding to the desired flow condition. If a non-steady state inflow is desired, velocity as a function of time can be implemented. For a tidal flow boundary, a function specifying the water surface elevation at the boundary can be applied. If no velocity or elevation is specified at cells, which terminate at the grid edge, they become no-flow boundaries in the algorithm.

2.2.4 Flow Model Input/Output Parameters

The area and bathymetry grids described in Section 2.2.2 are required to specify the domain to be modeled. Other required inputs are the tidal forcing function at the seaward boundary, the calculation time step, the total simulation time, a file containing Manning's n coefficient values for each cell, and velocities at the tributary flow boundaries. The output is three matrices consisting of the water surface elevations, x-direction velocities, and y-direction velocities, for every time step in the simulation.

2.3 Modeling Sediment Removal

2.3.1 Flow Model Input/Output Parameters

The accurate prediction of suspended sediment transport in estuaries is important for activities such as dredging, the accurate mapping of navigation channels and improved understanding of pollutant transport. The difficulty in formulating accurate suspended sediment transport formulas suitable for a range of input conditions arises because the sediment transport

forms a complex feedback system with the near-bed hydrodynamics and the bed topography. One important area of research related to the accurate prediction of suspended sediment transport is the formulation of the magnitude and shape of the temporally averaged suspended sediment concentration profile in a tidal channel. This subject is of practical importance, as the product of the temporally averaged suspended sediment concentration and horizontal velocity profiles form the dominant component of the horizontal suspended sediment flux in tidal and steady flow conditions (Rose and Thorne, 2001).

The sediment removal will use a 2D MATLAB based horizontal depth-averaged fine sediment transport model with the capability to manipulate erosion and deposition functions based on organic content. Initially the model hydrodynamics are determined by a finite difference semi-implicit algorithm developed by Casulli (1990). In this, the water surface elevation is obtained implicitly and the velocity is determined in an explicit fashion.

2.3.2 Governing Advection-Diffusion Equation

Advection-diffusion is calculated with Equation (2.6) using a finite-volume explicit method based on the quadratic upstream (QUICKEST) method of Leonard (1977) (Marvan et al., 2001):

$$\frac{\partial hC}{\partial t}+\frac{\partial (huC)}{\partial x}+\frac{\partial (hvC)}{\partial y}-\frac{\partial}{\partial x}\left(D_{xx}\frac{\partial hC}{\partial x}+D_{xy}\frac{\partial hC}{\partial y}\right)+\frac{\partial}{\partial x}\left(D_{yx}\frac{\partial hC}{\partial x}+D_{yy}\frac{\partial hC}{\partial y}\right)=S \quad , \qquad (2.6)$$

where t is time, C is the depth-averaged suspended sediment concentration, u and v are the longitudinal and transversal depth averaged velocities, h is the water depth and S is a source-sink term. The dispersion coefficients D_{xx}, D_{xy}, and D_{yy} are treated as follows (Preston, 1985):

$$D_{xx}=\frac{K_l u^2+K_t v^2}{C_z\sqrt{u^2+v^2}}h\sqrt{g} \qquad (2.7)$$

$$D_{yy} = \frac{K_l v^2 + K_t u^2}{C_z \sqrt{u^2 + v^2}} h\sqrt{g} \tag{2.8}$$

$$D_{xy} = D_{xy} = \frac{(K_l - K_t)uv}{C_z \sqrt{u^2 + v^2}} h\sqrt{g} \tag{2.9}$$

where K_l and K_t are the dispersion coefficients in the longitudinal and transversal directions taken to be 13 and 1.2 respectively, C_z is the Chey coefficient and g is the acceleration due to gravity. The source-sink term in Equation (2.6) accounts for the erosion and deposition in the following way:

$$S = Q_e + Q_d \tag{2.10}$$

where Q_e is the erosion flux at every time step and Q_d is the corresponding deposition flux.

2.3.3 Deposition Flux

The deposition flux is expressed according to Krone (1962) as:

$$Q_d = -pW_s C \tag{2.11}$$

where W_s is the sediment settling velocity and p is the probability for deposition defined as:

$$p = \left(1 - \frac{\tau_b}{\tau_d}\right) \tag{2.12}$$

where τ_b the bed shear stress and τ_d a critical shear stress for deposition. In this analysis, the parameter τ_d is set to a value above the highest shear stress found in the modeled domain, thus allowing deposition to occur at all times as long as suspended sediment is present.

Generally, the settling velocity of fine sediment is dependent on concentration. As a result, the settling velocity differs depending on three identifiable regimes: free settling, flocculation settling, and hindered settling. In the free settling range, relatively low concentrations permit the individual flocs to settle without interference from other flocs. The

settling velocity in this range is a function of the drag coefficient and the submerged weight of the floc. As concentration increases, the collision frequency of flocs increases, resulting in the formation of larger flocs. These flocs are able to settle quicker due to their increased mass, and characterize the flocculation settling range. Eventually, the concentration in the water column reaches a point where a floc is unable to settle quickly due to significant interference from other flocs, and the limited pore space for the fluid. This interference reaches a maximum when the water column resembles a bed of mud with negligible settling (Mehta, 1994). Hwang (1989) formulated a fit of the flocculation and hindered settling ranges, relating settling velocity to concentration as follows:

$$W_s = \frac{aC^{n_w}}{\left(C^2 + b^2\right)^m} \tag{2.13}$$

where a, b, m, and n_W are empirical constants. For the free settling range, at concentrations ($C \leq 0.25$ kg/m^3) a constant settling velocity (W_{sf}) is provided. Laboratory tests performed in a settling column are required to determine the site-specific constants. The settling velocity of the aggregates is a function of concentration and of shear stress, because the aggregation of particles depends on the number concentration of particles in the flow, but their ultimate size is limited by turbulent shearing (Mehta and Dyer, 1990).

2.3.4 Suspended Sediment Boundary Conditions

The boundary conditions at the tributary connections can be expressed as steady-state concentrations, or sediment rating functions can be applied if unsteady tributary flows are desired. This also holds true at the tidal entrance, where incoming concentrations can be specified, varying with tidal stage and/or current velocity.

2.3.5 Erosion Flux

In contrast to τ_d, Q_e cannot be treated in this way because erosion depends on the shear strength of the soil and is therefore considered in the following form:

$$Q_e = \varepsilon_N(\tau_b - \tau_s) \tag{2.14}$$

where ε_N is the erosion rate constant and τ_s is the bed shear strength. The bed shear stress is computed as

$$\tau_b = \frac{\rho_w g n^2 U^2}{(H+\eta)^{1/3}} \tag{2.15}$$

where ρ_w is the density of water. The shear strength of the bed is calculated via Mehta and Parchure (2001):

$$\tau_s = \alpha_s(\phi - \phi_s)^{\beta_s} \tag{2.16}$$

where ϕ is the solids volume fraction (ρ_D/ρ_s), ρ_D is the dry density, ρ_s is the grain density, ϕ_s is the limiting solids volume fraction value of ϕ at which $\tau_s = 0$ and α and β_s are sediment-specific empirical coefficients.

2.5 Sedimentation, Sediment Trap, and Trap Efficiency

2.5.1 Sedimentation

Sedimentation at any point in the estuary can be calculated from the deposit thickness Δh given by

$$\Delta h = \sum_{i=1}^{\frac{t_S}{\Delta t}} \frac{Q_{d_i}\Delta t}{\rho_d} \tag{2.17}$$

where t_s is the total simulation time, Δt is the time step, i is the time step index, Q_{di} is the deposition flux, and ρ_d is the deposit dry density. The sedimentation rate is then calculated by

$$S_R = \frac{\Delta h}{t_s} \tag{2.18}$$

where S_R is the sedimentation rate.

It is well known that in rapidly moving waters, fine particles are not deposited. Consequently, consideration must be made that sedimentation increases as flow velocity decreases. Since there is a close relationship between flow velocity and bottom shear, the following hypothesis has been proposed: shear stress in moving waters is an important controlling (reducing) factor on sedimentation. In aquatic systems, there are cohesive and noncohesive particles. The theoretical basis of cohesive material sedimentation in moving waters was derived from the fundamental flume experiments of Partheniades (1965, 1972). These experiments showed that sedimentation, as well as resuspension, depend on bottom shear stress. There are threshold values, one for sedimentation and a much higher value for resuspension. It was found that the degree of deposition (the proportion of the initially resuspended material, which settles) as well as the rate of deposition is controlled by the bottom shear. Partheniades (1972) wrote: "We may distinguish two groups of flocs: those with sufficient high strength to resist the flow induced disruptive shear stresses, which are highest near the bed, and those with insufficient strength. The first will be able to reach the bed, will develop several bonds with it and will become a part of it; the remaining flocs will be disrupted and reentrained" (Kozerski and Leuschner, 1999).

2.5.2 Definition of Trap

In this study, a sediment trap is defined as an area of the submerged bottom deepened to a depth greater than the surrounding bottom, in order to reduce flow velocity. The lower velocity should allow sediment to deposit in the trap rather than move past and deposit elsewhere. This in

turn allows for maintenance dredging to be performed at a specific location (the trap) rather than over a broad submerged area.

2.5.3 Definition of Trap Efficiency

Trap efficiency is defined as the percent by which effluent suspended sediment load is reduced with respect to the influent suspended sediment load (removal ratio). In a tidal situation, the seaward edge of the trap will be the influent side during flood tide, and the effluent side during ebb tide, and vice versa for the landward edge.

2.5.4 Calculation of Trap Efficiency

At each time-step in the sediment transport simulation the concentration, the velocity, and the water surface elevation will be calculated in each cell. The cells that border the trap and are flow-normal are also of interest. Sediment loads can be calculated for these border cells as follows:

$$q = UCH\Delta x \tag{2.19}$$

where q is the sediment load, U is the flow velocity, and Δx is the cell width. The sediment load on each side of the trap will be used to compute the sediment removal ratio as follows:

$$R = \frac{q_i - q_e}{q_i} \tag{2.20}$$

where R is the removal ratio, q_i is the influent sediment load, and q_e is the effluent sediment load. The removal ratio will be averaged over a tidal cycle, using the removal ratio values from each time-step.

2.5.5 Calculation of Trap Efficiency as a Function of Discharge

Simulations will be run for different discharges of the Cedar River. The average removal ratio for each trap will be compared for a given flow discharge. The normal flow will be used as the benchmark by which the efficiency of the trap will be assessed under the other discharge

cases. The removal ratio as a function of discharge will be plotted to determine what effect discharge has on trap efficiency.

CHAPTER 3
CEDAR, ORTEGA, AND ST. JOHNS RIVER SYSTEM

3.1 History and Description of the System

Before European involvement in North America, the Timucuan Indians called the St. Johns River Welaka, or river of lakes. In the early 1500s, Spanish seamen called the river Rio de Corrientes or River of Currents. In 1562, almost 50 years before the settlement in Jamestown, the French established Fort Caroline on a high bluff overlooking a river they called Riviere de Mai (River of May) because they arrived there on May 1. In 1565, Spanish soldiers marched north from St. Augustine, captured Fort Caroline and slaughtered the French. The Spanish renamed the river San Mateo to honor the saint whose feast followed the day they captured the river. Later, the river was renamed Rio de San Juan after a mission near its mouth named San Juan del Puerto. The English translation of the name Rio de San Juan, St. Johns River, lasted through English, Confederate and American possession of the river and remains today. Soon after England acquired Florida in 1763, King George III sent botanist John Bartram to explore Florida. His son, William Bartram, stayed in Florida and published his book Travels in 1791. It describes his exploration of the river as far south as Lake Harney. In the 1800s, steamboats made the St. Johns River a popular winter destination for northerners. By the 1860s, several steamers were making weekly round trips from Charleston and Savannah to Jacksonville and Palatka, and other settlements. In the 1900s, miles of floodplain were drained to make room for indigo, sugar cane, citrus and other profitable crops. Encroachment through draining of the headwater marshes at the river's southern end was neither planned nor controlled. More than 70 percent of the marsh was claimed for agricultural and urban uses. In 1954, Congress authorized flood-control works in the

southern part of the St. Johns River. To store water and to move floodwaters, large reservoirs and canals were designed by the U.S. Army Corps of Engineers. The Corps' project was halted in the 1970s. In 1974, the project was deemed unacceptable for environmental reasons. In 1980, a redesigned project by the St. Johns River Water Management District favored restoring wetlands to hold and release floodwaters and managing water levels to simulate natural marsh conditions. Since the project began, the District has restored more than 610 km^2 of original marsh, an area about the size of Delaware.

The St. Johns River is an ancient intracoastal lagoon system. As sea levels dropped, barrier islands became an obstacle that prevented water from flowing east to the ocean. The water collected in the flat valley and slowly meandered northward, forming the St. Johns River. The St. Johns River is the longest river in Florida at 500 km in length. The width of the river varies between a flat marsh at its headwaters and averages about two miles in width between Palatka and Jacksonville. In central Florida, the St. Johns River widens to form large lakes. Additionally, it is one of the few rivers in the United States that flows north. The total drop of the river from its source in marshes south of Melbourne to its mouth in the Atlantic Ocean near Jacksonville is less than 9 m, or about 1.6 cm per kilometer, making it one of the "laziest" rivers in the world. Because the river flows slowly, it is difficult for the river current to flush pollutants. Major pollution sources include discharges from wastewater treatment plants and stormwater runoff from urban and agricultural areas. This runoff carries pesticides, fertilizers and other pollutants into canals, ditches and streams that lead to the river with much of the river pollution is concentrated around urban areas. Salt water enters the river at its mouth in Jacksonville. In periods of low fresh water flow, tides may cause a reverse flow as far south as Lake Monroe, 260 km upstream from the river's mouth.

The Ortega River basin is located west of the St. John's River in south-central Duval county in northern Florida and is an important tributary of the St. Johns River (Figure 3.2). The Ortega River is the main tributary of the system, discharging approximately half of the total system's volume to the St. Johns River. The Cedar River is the second most important tributary and there are three other secondary tributaries of the system (Fishing Creek, Butcher Pen Creek and Williamson Creek). The upstream portion of the Ortega River is known as McGirt's Creek. The creek lies within the Duval uplands physiographic province and flows generally north to south. The Ortega River continues this course until it reaches the Eastern Valley physiographic province, where the river gradually turns 180 degrees to a north-northeasterly course before reaching the St. John's River north of the Jacksonville Naval Air Station.

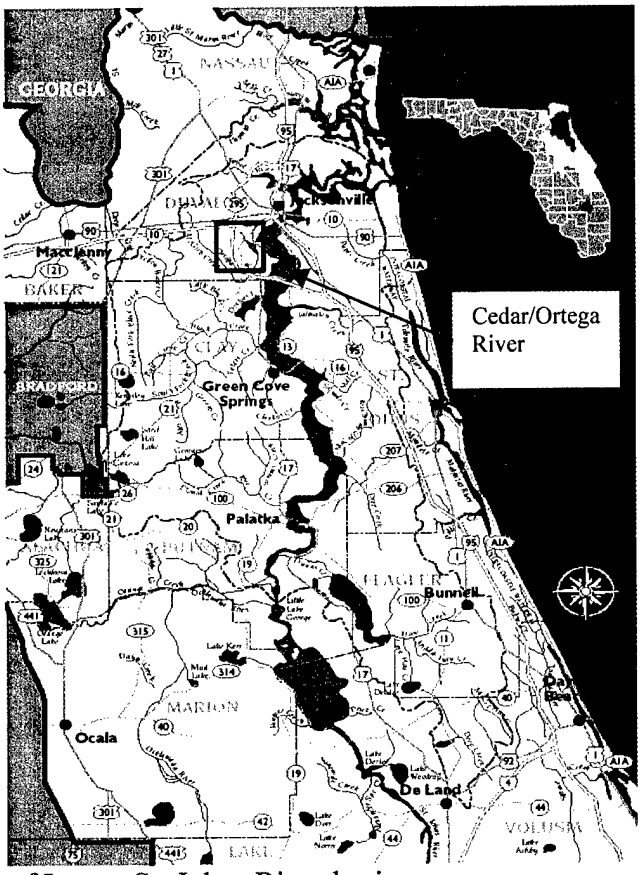

Figure 3.1 Regional map of Lower St. Johns River basin

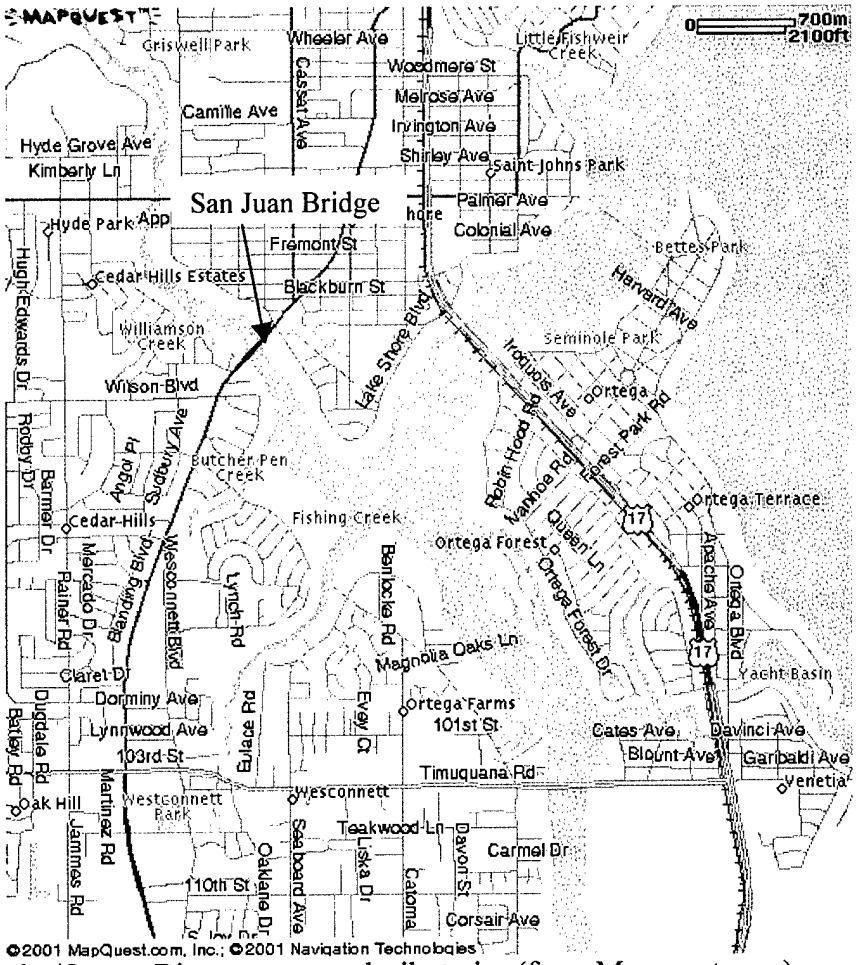

Figure 3.2: Cedar/Ortega River system and tributaries (from Mapquest.com).

The Cedar River, the largest tributary of the Ortega River (Figure 3.2), is actually a major system itself. From its head waters north of Interstate 10 and west if Interstate 295, this river flows southeast to its confluence with the Ortega River. Major tributaries to the Cedar River are Willis Branch, Williamson Creek, Butcher Pen Creek, and Fishing Creek. The tidal interface for the Ortega River is at Collins Rd., while the tidal interface for the Cedar River is near Lane Ave. (These two and other road locations are not highlighted in any drawings herin; they are found in road maps of the Jacksonville area.)

In the early 1990's, approximately one-third of the Ortega/Cedar River basin was residential, with commercial/industrial and vacant land comprising the other major land uses. Since then, vacant land has decreased significantly (Mehta et al., 2000). The average annual rainfall in the

Ortega/Cedar basin is approximately 132 cm and the major portion of it falls between June and September (Campbell et al., 1993). Water depths in the Ortega/Cedar basin study area range between 1 and 7 m, with the range in the Cedar River between 0.65 m and 4.3 m. At the mouth of the Ortega River with St. Johns River, the semidiurnal tide ranges from 0.14 m (neap tide) to 0.28 m (spring tide) having a mean of 0.19 m (this was the value used in the hydrodynamic model). The bottom and suspended sediment is mostly a mixture of clay, silt and organic matter. Typical suspended sediment concentration is approximately 15 mg/l; however, during storm runoff events it rises to as much as 105 mg/l. The mean organic content was found to be 28%. Previous samples from Mehta et al. (2000) show similar results for the sampled area having values between 22 and 36%. Measurements were also obtained from the St. Johns River Water Management District (SJRWMD), which showed less organic content ranging from 8-22% within the study area (Marván et al., 2000). For this analysis the mean organic content value will be used for calculation purposes.

CHAPTER 4
ASSESSMENT OF TRAP EFFICIENCY

4.1 Sediment Rating Relations

4.1.1 Sediment Rating Curve Definition

In many lowland rivers a major part of the sediment is transported in suspension. As the finest fraction of the suspended sediment load often is a non-capacity load it cannot be predicted using stream power related sediment transport models. Instead, empirical relations such as sediment rating curves often are applied. A sediment rating curve describes the average relation between discharge and suspended sediment concentration for a certain location. The most commonly used sediment rating curve is a power function (e.g. Walling, 1974, 1978):

$$C = aQ^b \tag{4.1}$$

where C is suspended sediment concentration (kg/m^3), Q is water discharge (m^3/s), and a and b are regression coefficients. Equation 4.1 covers both the effect of increased stream power at higher discharge and the extent to which new sources of sediment become available in weather conditions that cause high concentrations are related to the statistical method used to fit the sediment-rating curve and to the scatter about the discharge. Despite its general use several problems are recognized that regard the accuracy of the fitted curve as well as the physical meaning of its regression coefficients. Statistical inaccuracies related to the fitting procedure are discussed by Ferguson (1986, 1987), Jansson (1985), Singh and Durgunoglu (1989), and Cohn et al. (1992). They concluded that the sediment load of a river is likely to be underestimated when concentrations are estimated from water discharge using least squares regression of log-transformed variables. Scatter, among other things, caused by variations in sediment supply due to, for instance, seasonal effects, antecedent conditions in the river basin, and differences in

sediment availability at the beginning or the ending of a flood. This is not accounted for by the rating curve. As a sediment rating curve can be considered a 'black box' type of model, the coefficients a and b in equation 4.1 have no definite physical meaning. Nevertheless, some physical interpretation is often ascribed to them. Peters-Kümmerly (1973) and Morgan (1995) state that the a-coefficient represents an index of soil erosion severity. High a-values indicate intensively weathered materials, which can easily be eroded and transported. According to Peters-Kümmerly (1973), the b-coefficient represents the erosive power of the river, with large values being indicative for rivers where a small increase in discharge results in a strong increase in erosive power and sediment transport capacity of the river. Others state that the b-coefficient indicates the extent to which new sediment sources become available when discharge increases. Several authors compare the values of the b-coefficient obtained for different rivers to discuss differences in sediment transport characteristics in the different basins (Peters-Kümmerly, 1973; Walling, 1974; Sarma, 1986; Morgan, 1995; Kern, 1997).

As discussed previously, the values of the regression coefficients of sediment rating curves are assumed to depend on the severity of erosion, or the availability of sediment in a certain area, the power of the river to erode and transport the available material, and on the extent to which new sediment sources become available in weather conditions that cause high discharge. According to Walling (1974) b-values are also affected by the grain size distribution of the material available for transport, i.e. in streams characterized by sand sized sediments the power of the stream to transport sediment will be more important than in streams that mainly transport silt and clay. This will result in high b-values. However, as the a- and b-coefficients of sediment rating curves are inversely correlated (Rannie, 1978; Thomas, 1988) it seems more appropriate to use the steepness of the rating curve, which is a combination of the a- and b-

values, as a measure of soil erodibility and erosivity of the river. Steep rating curves, i.e. low *a*- and high *b*-values, should thus be characteristic for river sections with little sediment transport taking place at low discharge. An increase in discharge results in a large increment of suspended sediment concentrations, indicating that either the power of the river to erode material during high discharge periods is high, or that important sediment sources become available when the water level rises.

Flat rating curves should be characteristic for river sections with intensively weathered materials or loose sedimentary deposits, which can be transported at almost all discharges. When this line of reasoning is accepted for the Cedar River, the following interpretation can be assigned to the rating curves shown in Figure 4.3. This suggests a limited amount of fine sediment, which can be picked up from the bed at low discharge. Once a certain discharge threshold is exceeded, sediment supply to the river increases, and sediment can be picked up from the riverbed, resulting in a rapid increase in suspended sediment concentrations. This argument leads to the hypothesis that steeper rating curves are indicative of rivers, or river sections, where most of the sediment transport takes place at high discharge. Sediment transport rates estimated using a sediment-rating curve always differ somewhat from measured sediment loads. Hence, the sediment-rating curve produces only reasonable estimates of long-term total sediment loads. (Asselman, N.E.M., 2000).

4.2 Determination of Rating Curve

In the original analysis performed by Marván (2001), the number of suspended sediment measurements were limited, hence, in order to set the boundary conditions for the tributaries a rating curve was developed by relating the peak and mean values of concentration C to the

corresponding peak and mean river discharge Q in the Ortega and Cedar rivers, obtaining the following relations (Fig. 4.1).

$$C = 2 \times 10^{-5} Q^{2.23} \tag{4.2}$$

At the mouth of the Ortega river, this boundary condition was only applied when the flow was entering the system from St. Johns River. Since no concentration data were available from this site, by using the sediment characteristics and a zero-dimensional resuspension model (Mehta and Li, 1999) the following rating curve was developed for the Cedar river:

$$C = 1.65 \times 10^{-2} Q^{0.52} \tag{4.3}$$

At the time of Marván's analysis, only limited data were available. Further analysis was performed to validate the Cedar River rating curve utilizing additional data from the SJRWMD. The additional discharge data were included with original data and averaged by month and plotted against the concentration, the resulting data were band averaged to reduce scatter. A new rating curve was fit to the band averaged data as shown in Figure 4.1. Following is the recalculated rating curve for the Cedar River:

$$C = 6 \times 10^{-2} Q^{0.28} \tag{4.4}$$

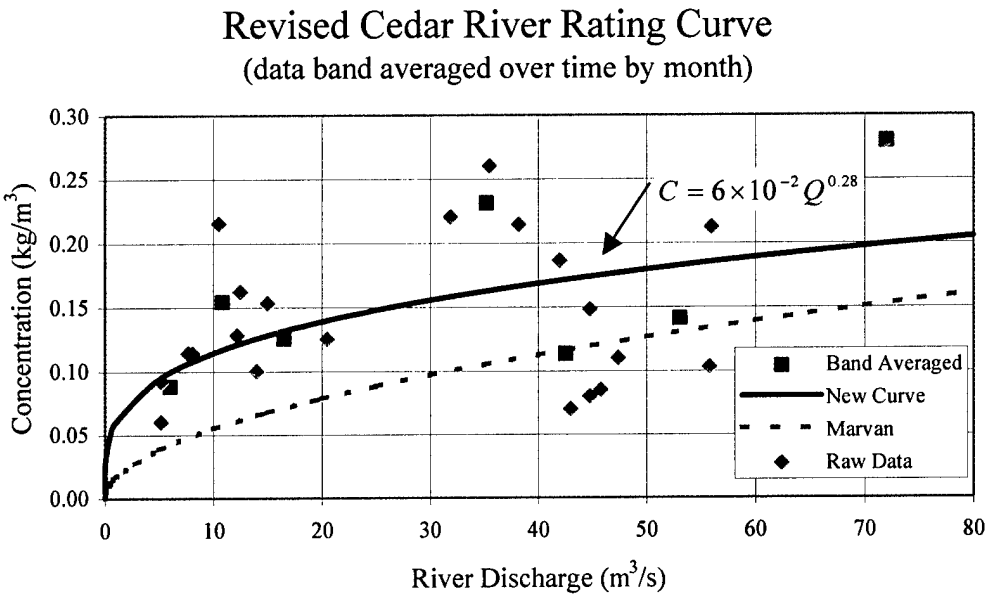

Figure 4.1 Revised Cedar River sediment rating curve.

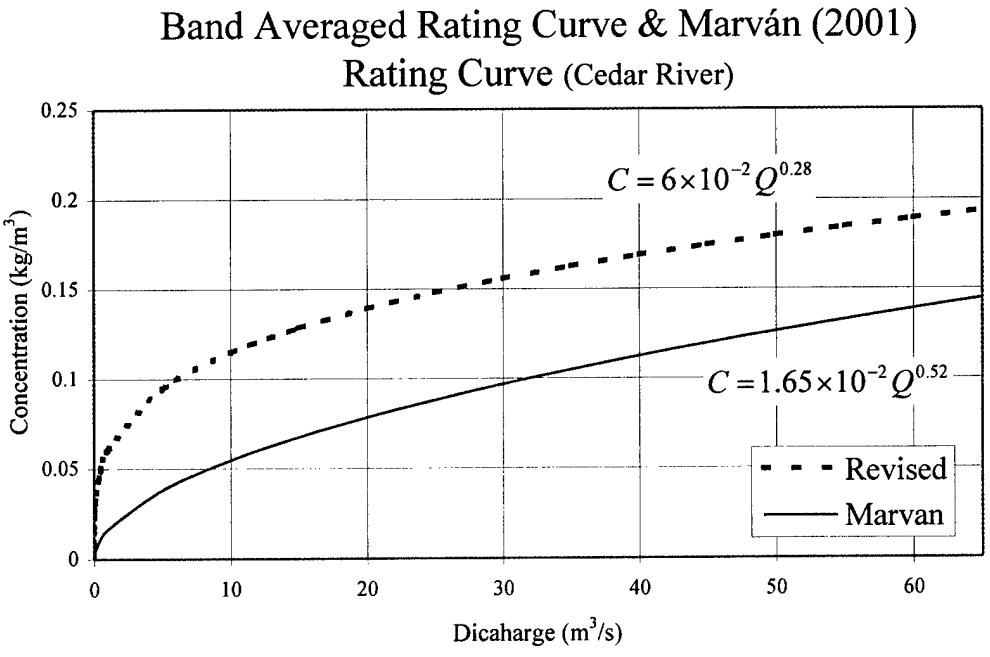

Figure 4.2 Comparison between Marván (2001) and new Cedar River sediment rating curves.

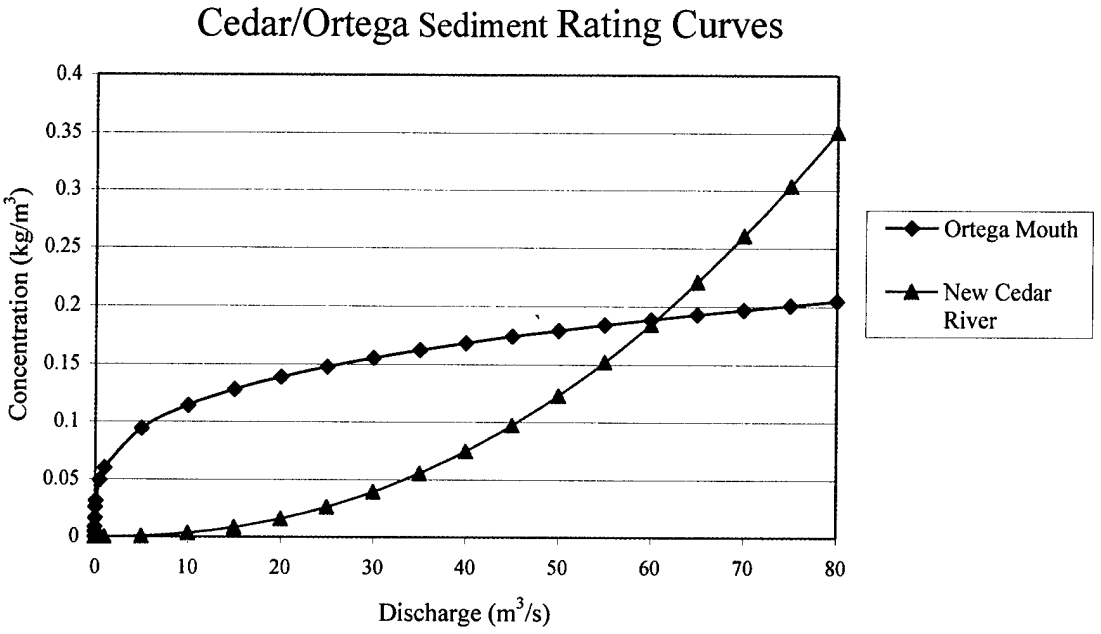

Figure 4.3 Cedar/Ortega River sediment rating curves.

Figure 4.2 shows a comparison between the original Cedar River rating curve and the revised curve. The new curve values were incorporated in to the sediment model. Figure 4.3 shows the sediment rating curves for the Cedar/Ortega system that serve as sediment concentration boundary conditions for the sediment transport model.

4.3 Trap Design Selection

4.3.1 Factors and Considerations

Some basic design factors were considered in sizing and locating the traps. The following are some basic factors as Parchure et al. (2000) indicates to consider when designing a sediment trap:

a. Locate the trap at a place of maximum sediment transport.

b. It should have navigational access for a dredge to get in and get out without difficulty.

c. The depth and size of the trap should permit safe operation of a dredge.

d. The storage volume of the trap should permit adequate temporary storage of the sediment.

e. Preferably, the trap should catch both fine and coarse sediment.

f. The prevailing flow pattern should be approximately normal to the longer side of the trap.

These factors were evaluated and applied in varying degrees when selecting the size and location of the test traps.

4.3.2 Evaluation

Based on flow data and previous hydrodymanic and sediment transport analyses of the Cedar River system by Marván et al. (2000) and Mehta et al. (2000), Trap 1 is placed near the confluence of the Cedar and Ortega Rivers. Trap 2, conversely is located approximately 420 m upstream. Both traps were selected 60m (1 cell) wide by 300m (5 cells) long with a surface area of 18,000 m^2 and a volume of 36,000 m^3. The traps are to have an initial dredged depth of 2 meters (from original bed depth) of the river cross-section, which for Trap 1 the dredging depth is 3.8 m and the dredging depth for trap 2 is 3.2 m. These were considered sufficient to reduce the velocity in the canal to allow measurable sediment to settle. For example, with a flow of 3 m^3/s and regular tidal forcing in the Cedar River, the average velocity over trap 1 was found to be 0.13 m/s. Over the same location with no trap in place, the average velocity was 0.24 m/s, which results in a 49% reduction in velocity over the trap. The range of velocity reduction for trap 1 and trap 2 were from 44% to 51% and 43% to 53%, respectively with an overall average velocity reduction of 48%.

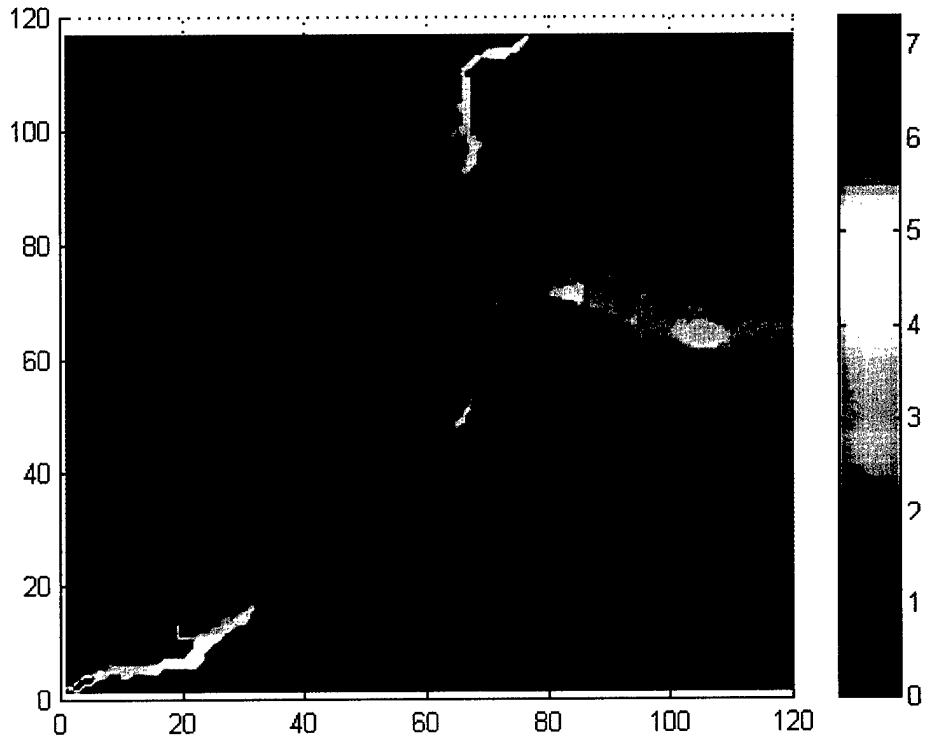

Figure 4.4 Bathymetry of Cedar/Ortega River as used in hydrodynamic/sediment transport models.

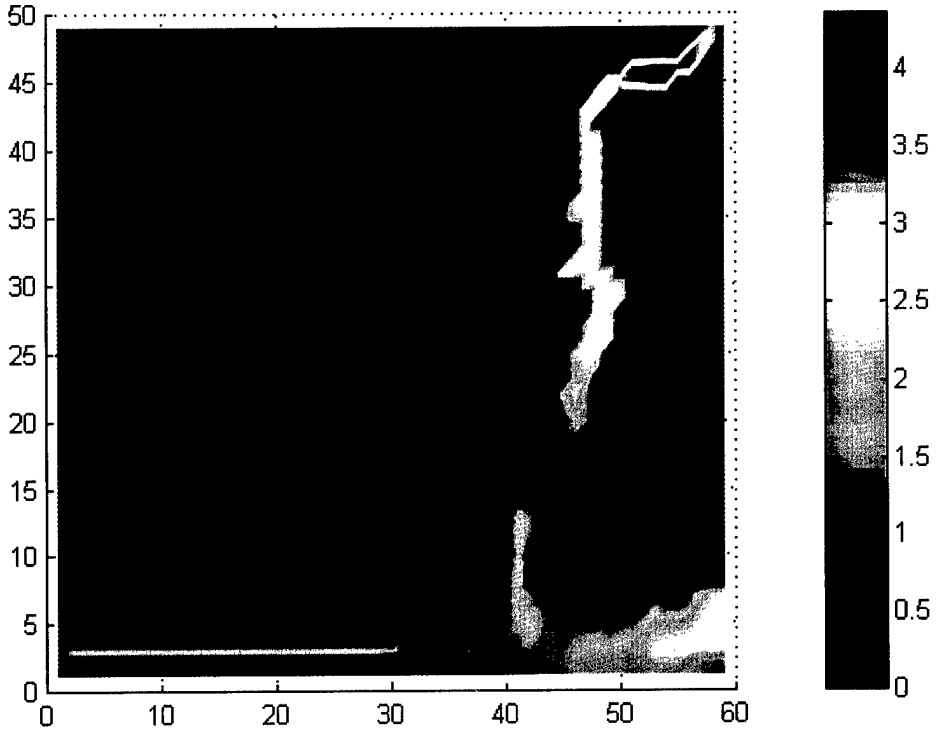

Figure 4.5 Bathymetry of Cedar River as used in hydrodynamic/sediment transport models.

In order to correctly incorporate the trap into the computer model, the existing bathymetry file was updated with the location and depths of the traps at the selected cells. The output from the flow model was then input into the sediment transport model. Sediment removal ratio, as defined by Equation 2.20, was calculated from the influent and effluent sediment loads in units of kg/s (Equation 2.19) at the cells adjacent to the trap on the upstream and downstream edges of the trap. The input densities (dry, bulk, granular) required for the trap were determined from Figure 4.6, and the values are 157 kg/m^3, 1099 kg/m^3, 2188 kg/m^3, respectively.

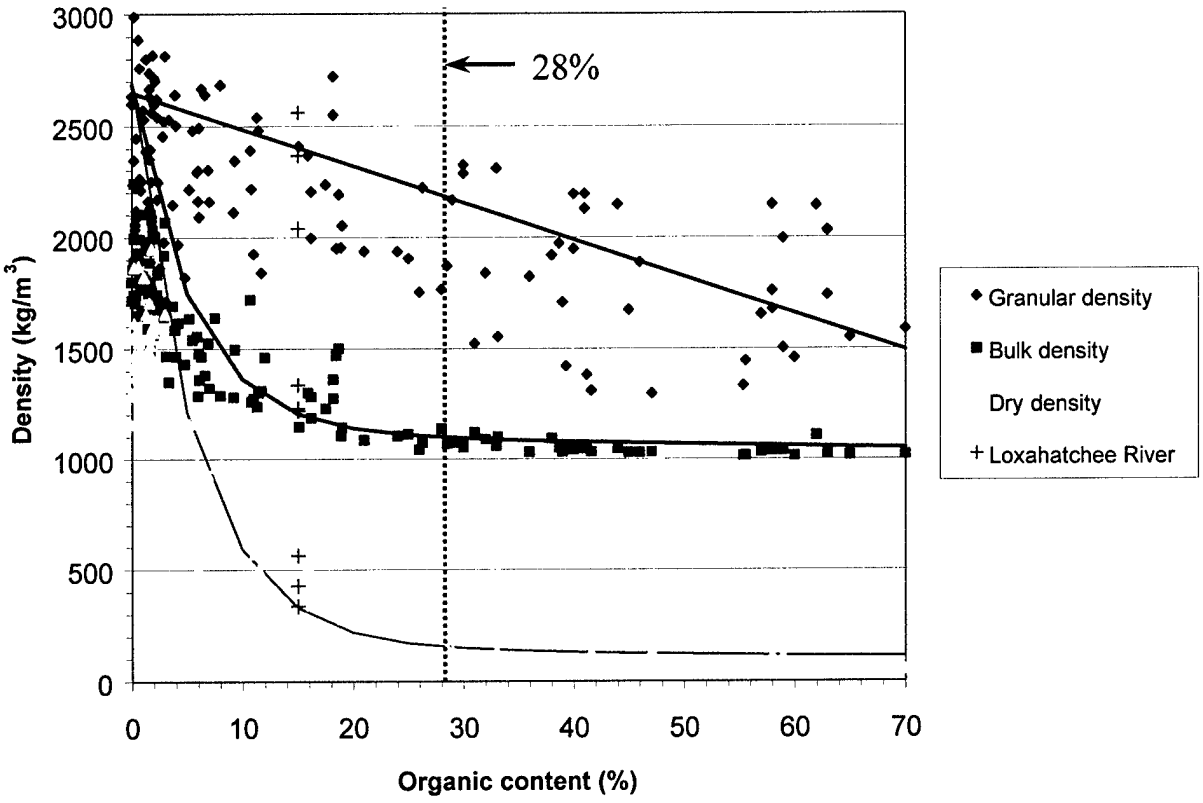

Figure 4.6 Variation of granular, bulk, and dry densities with organic content using data from three Florida locations and the Loxahatchee River (from Ganju, 2001).

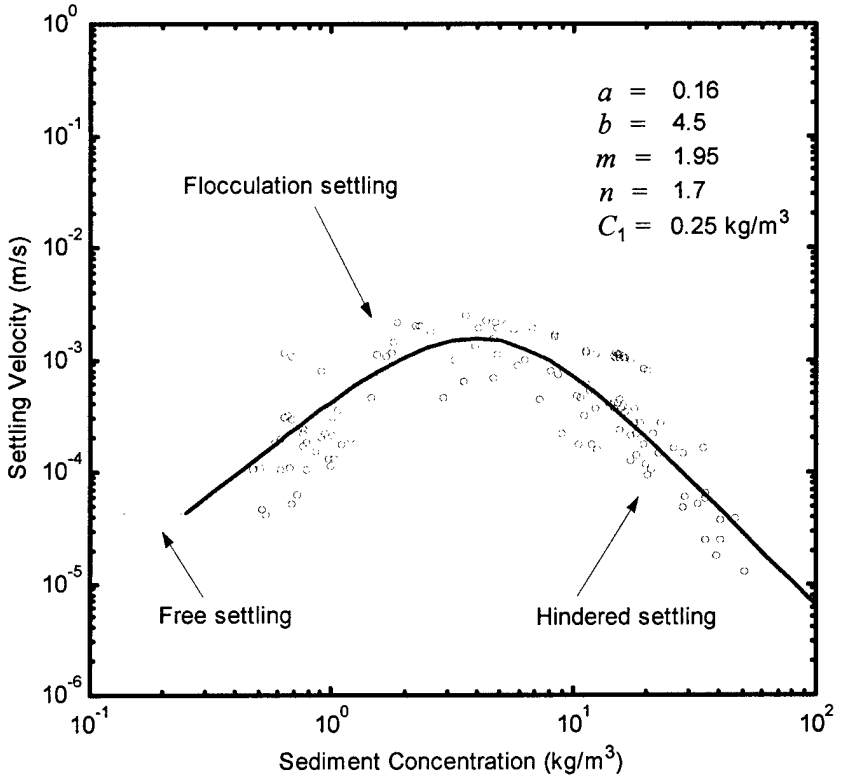

Figure 4.7 Settling velocity vs. sediment concentration.

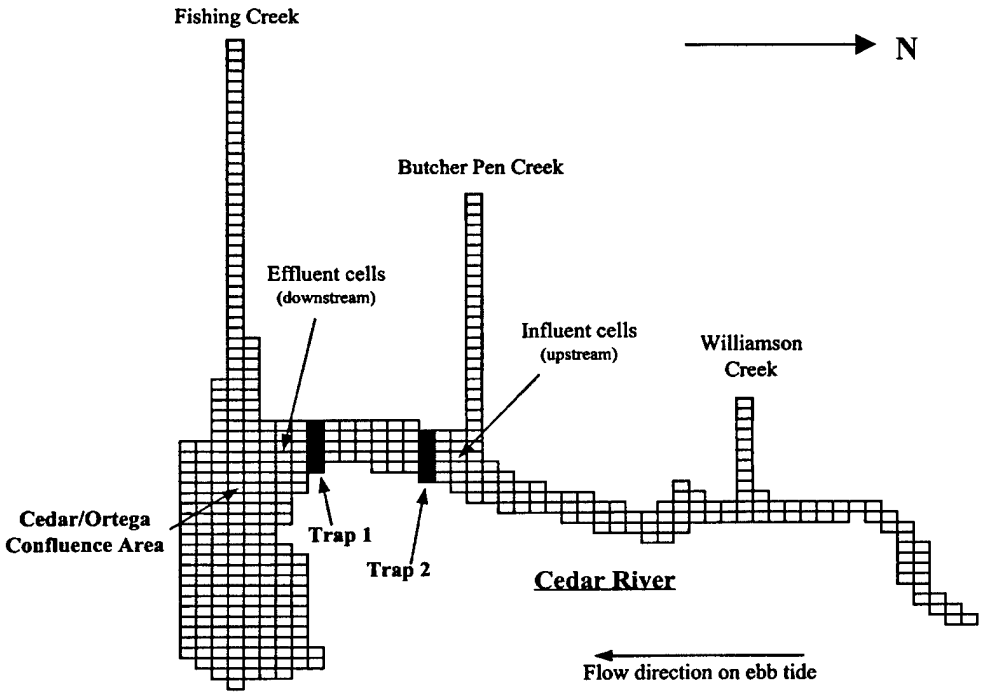

Figure 4.8 Cedar River section of the computational grid. (Trap cells are shown in black.)

Influent and effluent sediment loads were calculated for each time step, and then the removal ratio averaged over one ebb tidal cycle as follows:

$$R_{ave} = \frac{\sum_{i-1}^{M} R_i}{M} \tag{4.5}$$

where R_{ave} is the ebb tide averaged removal ratio, i is the index for each time step Δt, R_i is the removal ratio from a single time step, and M is the total number of time steps over a complete tidal period, as follows:

$$M = \frac{T}{2\Delta t} \tag{4.6}$$

where T is the tidal period (12.42 h). Flood tidal data were not used to calculate the removal ratio because the effluent load (downstream edge) contained only the sediment which escaped the trap on the previous ebb tide. It was observed that for 63% flow (35.4 m^3/s) was the only discharge that produced a constant flow toward the St. Johns River even while the tide was flooding although small flood values appeared at a discharge of 16.4 m^3/s. For the 35.4 m^3/s flow, the removal ratio was calculated for the entire tidal period.

4.4 Trap Efficiency as a Function of Discharge

4.4.1 Trap Performance

Harmonic analysis was carried out by Marván (2001) for tide at the Ortega River mouth at the St. Johns River in order to generate a one-year water level record. Water surface elevation and velocity data from San Juan Bridge (Fig. 3.2) provided by SJRWMD was used for calibration of the hydrodynamic model. River discharge was also available in Ortega River having a mean discharge of 1.4 m^3/s and a maximum of 112 m^3/s. By measuring the watersheds of the other main tributaries (Fishing Creek, Butcher Pen Creek, Williamson Creek and Cedar River), an estimate of the river discharge was made, yielding the rates given in Table 4.1.

Table 4.1. – Cedar/Ortega and tributary discharges in m^3/s

Tributary	Normal conditions	Storm runoff event
Ortega River	$8.50x10^{-1}$	$7.80x10^{1}$
Fishing Creek	$1.60x10^{-1}$	$1.46x10^{1}$
Butcher Pen Creek	$4.00x10^{-2}$	$3.75x10^{0}$
Williamson Creek	$3.90x10^{-2}$	$3.64x10^{0}$
Cedar River	$6.50x10^{-1}$	$5.52x10^{1}$

(From Marván et al., 2001)

The hydrodynamic and sediment transport models used were previously calibrated as discussed in Marván et al. (2000) and utilized for the trap analysis. Using the calibrated model, several discharges were used for evaluation. Table 4.2 provides the evaluation discharges and associated concentrations using the recalculated Cedar River rating curve. Due to model limitations at the time of evaluation, the 100% discharge of 55 m^3/s was not evaluated. The organic content included in the model was 28%, which is the mean organic content of the Cedar River sediment. Removal ratios were calculated only during periods of ebb tide flow through the trap (Section 4.3), and plotted against Cedar River discharge (Figure 4.9) and velocity (Figure 4.10). These simulations show that the removal ratio is maximum at a discharge of approximately 16.4 m^3/s. At higher discharges the removal declines meaning that the velocity is too large to allow particles to settle in the trap and are subsequently transported past the trap. Conversely, at significantly lower discharges the same particles settle before arriving at the trap.

To provide a performance comparison, the trap was moved 420 m upstream from its previous location. The dredge depth and surface area of the trap remained the same at 18,000 m^2. The original bathymetric grid was adjusted to reflect the new depth. The removal ratio for Trap 2 was calculated for the same discharges. Table 4.2 compares the removal ratios for the discharges at each trap location. Trap 2 performed 28 % better at the peak removal ratio flow rate (16.4 m^3/s) and by an overall average of 56% over Trap 1. This reduced performance by Trap 1 can be

partly attributed to the increased tidal action near the confluence of the Cedar and Ortega Rivers where Trap 1 is located. Trap 2 performed more effectively due to more consistent flow direction and velocity since the location is well within the Cedar River. Trap 1, being closer to the Ortega River confluence area experienced more "mixing", reducing trapping efficiency.

Table 4.2 Removal ratio as a function of Cedar River discharge for Trap 1 and Trap 2

Cedar River Discharge (m^3/s)	Trap 1 Removal Ratio	Trap Removal Ratio
0.65	.09	.14
3.0	.18	.29
16.4	.27	.35
34.5	.15	.26

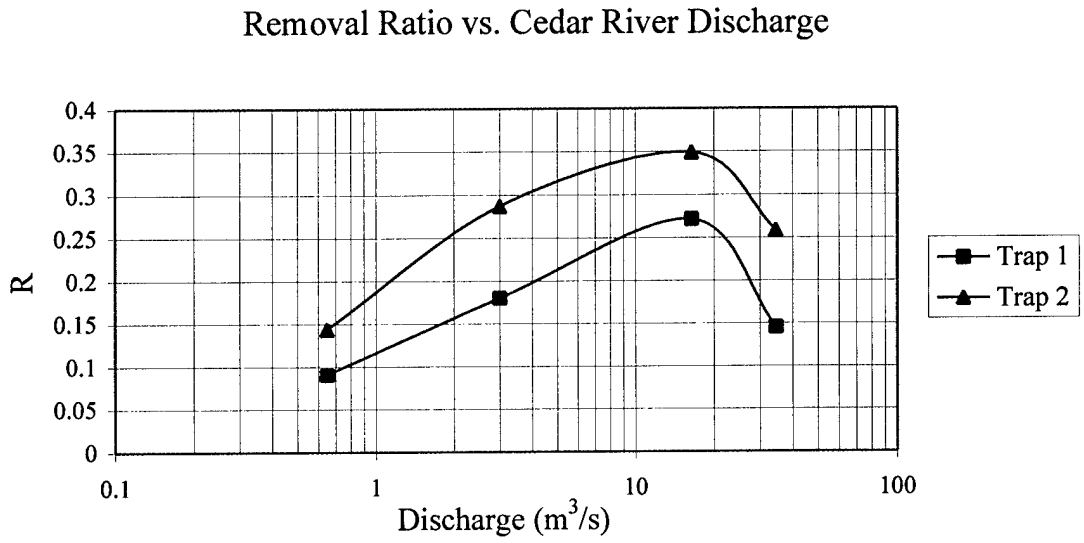

Figure 4.9 Removal ratio of trap 1 and 2 as a function of Cedar River discharge.

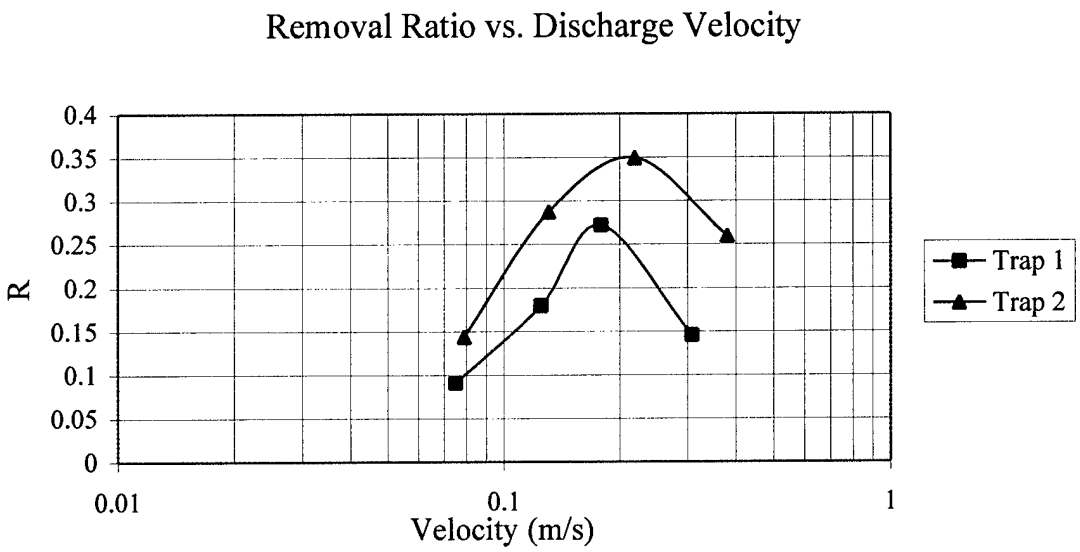

Figure 4.10 Removal ratio of trap 1 and 2 as a function of Cedar River velocity.

4.4.2 Tidal Influence on Performance

Similar to the results in Ganju (2000), the removal ratios for both traps increase until a critical discharge is reached and then decrease. For this system, each trap, the "break-even" discharge was 16.4 m^3/s. Considering the graphical removal ratio solution from Mehta (1984) for a basin with two entrances, the Cedar River trapping schemes results in the relationship

$$R \propto \frac{1}{U} \tag{4.7}$$

with settling velocity, trap length constant, the removal ratio is proportional to the discharge velocity. As verification, recalling the depositional flux is:

$$Q_d = W_s CL \tag{4.8}$$

and the total sediment flux entering the trap is

$$Qi = CUh \tag{4.9}$$

and taking the removal ratio as

$$R = \frac{q_i - q_e}{q_i} = \frac{Q_d}{Q_i} = \frac{W_s L}{Uh} \tag{4.10}$$

it can be shown to be proportional to U^{-1} since W_s, L, and h are essentially constant. Conceptually, as the velocity decreases, the removal ratio should increase. This theory is supported by Baker et al. (1988), but for both of these situations, the velocity was unidirectional. Baker et al. showed that for a sediment trap in a unidirectional flow the removal ratio increased as the velocity approached zero. For the chosen trap locations, as the discharge velocities decrease, tidal influences increase. Starting with the highest discharge (unidirectional flow) and working toward the minimum discharge (bi-directional flow), the removal ratio increases until a maximum value is reached for each trap. Traps 1 and 2 had maximum removal ratios of 0.27 and 0.35, respectively. Continuing to reduce the discharge from the peak removal ratio at 16.4 m^3/s, the tidal influences begin to appear changing the flow from unidirectional to bi-directional. As the discharge approaches zero the tidal forcing effect increases and becomes maximum, which keeps the sediment in the vicinity of the trap in a semi-resonant pattern for a longer period of time before being pushed through the system as in the unidirectional or runoff induced flow case.

Based on the results and observations thus far, it is believed that tidal influence is a contributing factor in removal ratio calculation and should be evaluated. In a unidirectional flow, the sediment is more likely to settle because external disturbances are reduced versus the directional velocity changes that take place in a bi-directional flow situation. By changing direction, some of the previously deposited sediment may become resuspended if consolidation has not occurred. If the discharge is minimal and tidal forcing is near maximum, the consolidation would be small and resuspension more likely. With this in mind, the removal ratio would decrease. Of course, actual sediment characteristics that would have to be evaluated for each system depends significantly on settling velocity. In this analysis, the settling velocity is

free settling and constant because the concentrations are small. Each estuarine system would have to be evaluated to determine the discharge value where tidal influence begins to impact removal ratio. A general relationship can be developed for both tidal and non-tidal influenced removal ratio portions.

As tidal influence increases, the equivalent trap length theoretically increases due to the resonance in the system. This tidal equivalent trap length (L) can be illustrated by using the following expression:

$$\frac{L}{L_o} = k\left(\frac{U}{U_o}\right)^m, \quad m > 1 \tag{4.11}$$

where L_o is the original trap length and U_o is a characteristic velocity of the non-tidal portion of the removal ratio (most likely for the desired evaluation discharge). The value m is a scaling factor to account for the varying tidal influences as the discharge changes. Substituting this expression into Equation 2.30 and converting the velocities into discharges, the following expression results for the tidal-influenced removal ratio:

$$R = \frac{W_s L_o B}{Q} k\left(\frac{Q}{Q_o}\right)^m = \lambda \frac{W_s L_o B}{Q}; \quad \text{where } \lambda = k\left(\frac{Q}{Q_o}\right)^m \tag{4.12}$$

where λ is the dimensionless tidal influence factor. Figure 5.2 shows the tidal/non-tidal influenced removal ratio using Equations 2.30 and 2.32 for k=1, m=1.5, and Q_o=5 m^3/s..

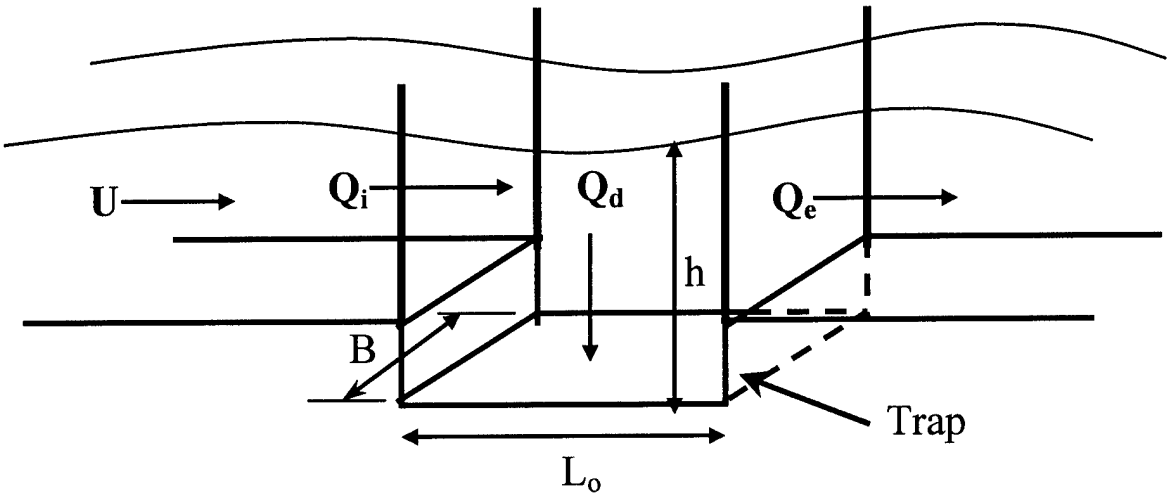

Figure 5.1 Single-Box model for illustration of tidal/non-tidal removal ratio as a function of deposition and erosion fluxes.

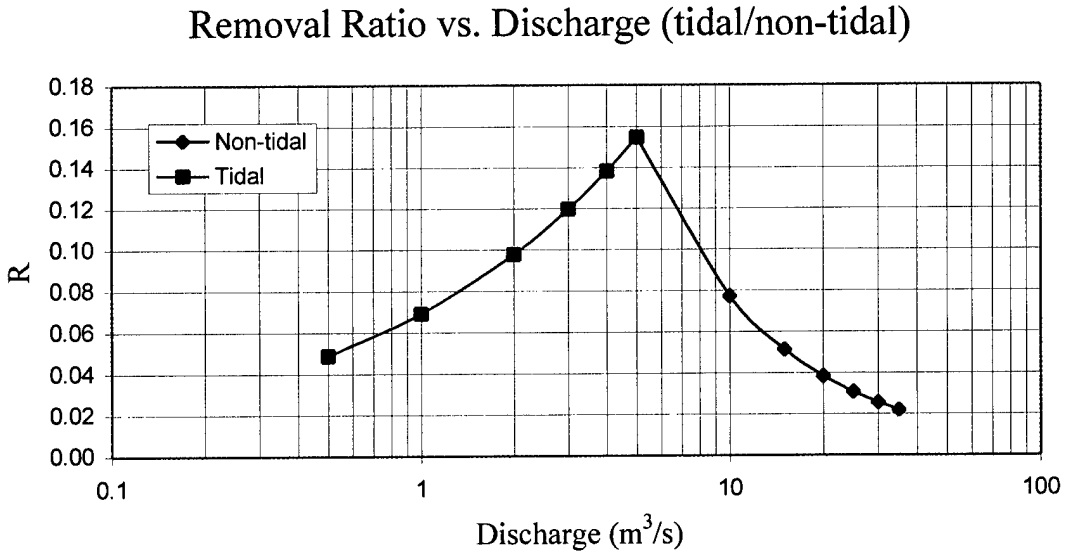

Figure 5.2 Tidal/Non-tidal removal ratio as a function of discharge

The resulting trend from Equation 4.12 is very similar to the model results verifying that a tidal influence that reduces the removal ratio is present at lower discharges. To ensure a valid and accurate application, the appropriate scaling factors (m and k) need to be adjusted for each system and trap configuration.

CHAPTER 5
CONCLUSIONS

5.1 Summary

The objective of this study was to determine the effect of discharge on trapping efficiency for a given trap design in different locations. The Cedar River was chosen as the location of the study due to the influx of organic rich fine sediment and contaminants from upstream sources desired to be kept in the traps rather than spread through the entire biologically sensitive estuarine system. Flow (hydrodynamic) and transport models were utilized to calculate the water levels, velocities, and sediment concentrations in the Cedar/Ortega River system. The models were calibrated using data previously collected from available sources and field investigations (see Marván, 2001). Tidal elevations and currents were measured, and historical tributary flow data were obtained from St. Johns River Water Management District (SJRWMD in order to calibrate the flow model.

Utilizing the calibrated model, a sediment trap in two locations was incorporated into each of the models to determine the trapping efficiency as a function of discharge. The results of these simulations and conclusions are discussed in the following section.

5.2 Conclusions

1) The simulations for trap efficiency as a function of Cedar River discharge demonstrate a specific discharge (16.4 m^3/s) at which the sediment removal ratio is a maximum. Above this discharge, particles are moving fast enough to bypass the trap and below this discharge the particles deposit before arrival at the trap. A comparison trap was evaluated 420 m upstream. The trap performed 28% better while maintaining the maximum removal ratio at 16.4 m^3/s.

2) Comparing the trapping efficiency results against the expected relationship for removal ratio, the inconsistencies appear at lower velocities. According to the theory, as velocity decreases the trapping efficiency increases since the removal ratio is proportional to U^{-1}. This indicated another influence was present in the system reducing the efficiency at lower velocities. Also noticed as the discharge velocities decreased, the tidal influence became stronger. A relationship was developed and applied to account for the increase tidal influence at lower velocities Equation 4.12.

5.3 Recommendations for Further Work

The trapping efficiency calculation would be more accurately performed with a 3-D model to more effectively account for the mud suspension in high concentrations just above the bed.

Prior to any full scale dredging, a test pit should be dredged to accurately determine sedimentation, flow velocity (to calculate discharge), pressure (to determine water elevation), and deposition thickness in the test pit in the Cedar River. A proposed trap is showed in Figure 5.1. The system setup would have a central data logger to record output from the turbidity meters, current meter, and pressure sensor. To determine the equilibrium bed elevation and the pit bed level, divers would be needed. A similar system was deployed by Harley and Dean (1982) off the coast of Colombia.

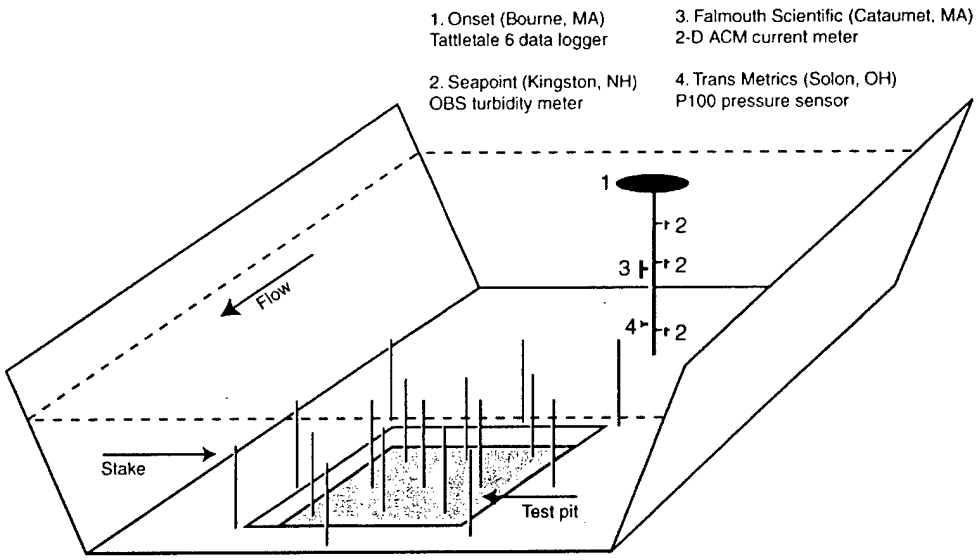

Figure 5.1 Possible layout of an experimental test pit from Ganju (2001).

Vicente (1992) provides a method to calculate a constant sedimentation coefficient (K), which can be used to calculate bed elevation through time, as follows:

$$H(t) = H_o + (H_h - H_o)(1 - e^{-Kt}) \tag{5.1}$$

where H(t) is the bed elevation at any time, H_o is a datum elevation, and H_e is the equilibrium bed elevation (in absence of dredging). In order to determine K, test pit bottom elevations must be recorded over time, referenced to H_e. Once the time/elevation data are recorded for different areas of the pit, K is determined. One benefit of this method is that only two monitoring visits are needed to determine K. Shoaling depth through time can then be estimated for the site, with the final shoaling depth approaching the equilibrium bed elevation (Ganju, 2001).

REFERENCES

Asselman, N.E.M., 2000. Fitting and interpretation of sediment rating curves. *Journal of Hydrology*, 234, 228-248.

Baker, E.T., Milburn, H.B., and Tannant, D.A., 1999. Field Assessment of sediment trap efficiency under varying flow conditions. *Journal of Marine Research*, 46, 573-592.

Campbell, D., Bergman, M., Brody, R., Keller, A., Livingston-Way, P., Morris, F., and Watkins,B., 1993. *Lower St. Johns river basin SWIM plan*. St. Johns River Water Management District.

Cancino, Leonor and Neves, Ramiro, 1999. Hydrodynamic and sediment suspension modeling in estuarine systems, Part I: Description of the numerical models. *Journal of Marine Systems*, 22, 105-116.

Casulli, V., 1990. Semi-implicit finite difference methods for the two-dimensional shallow water equations. *Journal of Computational Physics*, 86, 56-74.

Cohn, T.A., Caulder, D.L., Gilroy, E.J., Zynjuk, L.D., Summers, R.M., 1992. The validity of a simple statistical model for estimating fluvial constituent loads: an empirical study involving nutrient loads entering Chesapeake Bay. *Water Resources Research*, 28, 2353–2363.

Ferguson, R.I., 1986. River loads underestimated by rating curves. Water Resources Research 22, 74–76.

Ferguson, R.I., 1987. Accuracy and precision of methods for estimating river loads. Earth Surface Processes and Landforms 12, 95–104.

Ganju, N.K., 2001. Trapping Organic-Rich Fine Sediment in an Estuary. *Masters thesis*, University of Florida, Gainesville, Fl.

Ghosh, L.K., Prasad, N., Joshi, V.B., Kunte, K.K., 2001. A study on siltation in access channel to a port. *Coastal Engineering*, 43, 59–74.

Harley, R. and Dean, R.G., 1982. Channel shoaling prediction: A method and application. *Proceedings of the 18th International Conference of Coastal Engineering*, ASCE, 1199-1218.

Hwang, K., 1989. Erodibility of fine sediment in wave-dominated environments. *M.S. thesis*, University of Florida, Gainesville, FL, 166p.

Jansson, M., 1985. A comparison of detransformed logarithmic regressions and power function regressions. Geografiska Annaler 67A, 61–70.

Kern, U., 1997. Transport von Schweb- und Schadstoffen in staugeregelten Fließgewässern am Beispiel des Neckars. Mitteilungen Institut für Wasserbau, Universität Stuttgart, Stuttgart, Germany.

Kozerski, Hans-Peter and Leuschner, Klaus, 1999. Plate Sediment Traps For Slowly Moving Waters. *Water Resources*, 33, No. 13, pp. 2913-2922.

Krone, R.B., 1962. Flume studies of the transport of sediment in estuarial shoaling processes. *Final Report*, Hydraulics Engineering Laboratory and Sanitary Engineering Research Laboratory, University of California, Berkeley, CA, 118p.

Leonard, B.P., 1977. A stable and accurate convective modeling procedure based on quadratic upstream interpolation. *Computer Methods in Applied Mechanics and Engineering*, 19, 59-98.

Marván, F.G., Wallis, S.G., Mehta, A.J., 2001. Episodic Transport of Organic-Rich Sediments in a Microtidal Estuarine System. Research paper to be published in *Proceedings if INTERCOH 2000.*

Marván, F.G., 2001. A two-dimensional numerical transport model for organic-rich cohesive sediments in estuarine waters. *Ph.D. thesis*, Heriot-Watt University, Edinburgh, UK.

Mehta, A.J., Kirby, R., Stuck, J.D., Jiang, J., and Parchure, T.M., 1997. Erodibility of organic rich sediments: A Florida perspective. *Report UFL/COEL-99/019*, Coastal and Oceanographic Engineering Department, University of Florida, Gainesville, FL, 60p.

Mehta, A.J., Ariathurai, R., Peng-Yea, M., and Hayter, E.J., 1984. Fine Sedmentation in Small Harbors. *Report UFL/COEL-TR/051*, Coastal and Oceanographic Engineering Department, University of Florida, Gainesville, FL, 113p.

Mehta, A.J., Kirby, R., and Hayter, E.J., 2000. Ortega/ Cedar River basin, Florida, restoration: Work plan to assess sediment-contaminant dynamics. *Report No. UFL/COEL-99/019* Coastal and Oceanographic Engineering Department, University of Florida, Gainesville, FL, 30p.

Mehta, A.J. and Parchure, T.M., 2001. Surface erosion of fine-grained sediment revisited. In: *Muddy Coast Dynamics and Resource Management*, B.W. Flemming, M.T. Delafontaine, and G. Liebezeit, eds., Elsevier, Oxford, UK (in press).

Mehta, A.J. and Dyer, K.R., 1990. Cohesive Sedimant Transport in Estuarine and Coastal Waters. In: *The Sea (Vol. 9, Part B), Ocean Engineering Science*, B. Le Mehaute and D.M. Hanes, Wiley and Sons, New York.

Mehta, A.J., Lee, S.C., Li, Y., Vinzon, S.B., and Aberu, M.G., 1994. Analysis of some sedimentary properties and erodibility characteristics of bottom sediment for the Rodman Reservoir, Florida. *Report No. UFL/COEL-90/008*, Coastal and Oceanographic Engineering Department, University of Florida, Gainesville, FL.

Morgan, R.P.C., 1995. Soil erosion and conservation, 2nd ed. Longman, London.

Parchure, T.M., Brown, B., and McAdory, R.T., 2000. Design of Sediment Trap at Rollover Pass, Texas. *Report No. ERDC/CHL TR-00-23*, United States Army Corps of Engineers Coastal and Hydraulics Laboratory, Vicksburg, Mississippi.

Peters-Kümmerly, B.E., 1973. Untersuchungenüber Zusammensetzung und Transport von Schwebstoffen in einigen Schweizer Flüssen. Geographica Helvetica 28, pp. 137–151.

Pnueli, D. and Gutfinger, C., 1992. *Fluid mechanics*. Cambridge University Press, New York, 473p.

Preston, R.W., 1985. The representation of dispersion in two-dimensional shallow-water flow. *Report TPRD/L/2783/N84*, Technology Planning and Research Division, Central Electricity Research Laboratories, 13p.

Rose, C. P. and Thorne, P. D., 2001. Measurements of suspended sediment transport parameters in a tidal estuary. *Continental Shelf Research*, 21, pp. 1551-1575.

Sarma, J.N., 1986. Sediment transport in the Burhi Dihing River, India. In: Hadley, R.F. (Ed.). Drainage basin sediment delivery, *IAHS publication*,159, pp. 199–215.

Singh, K.P., Durgunoglu, A., 1989. Developing accurate and reliable stream sediment yields. *Sediment and the environment*, IAHS publication, Wallingford, 184 (Proceedings of the Baltimore symposium, May 1989: pp. 193–199).

Trefry, J.H., Chen, N.C., Trocine, R.P., and Metz, S., 1992. Impingement of organic-rich, contaminated sediments on Manatee Pocket, Florida. *Florida Scientist*, 55(3), 160-171.

Vicente, C.M.,1992. Experimental dredged pit of Ka-Ho. Analysis of shoaling rate. *Proceedings of the International Conference on the Pearl River Estuary*, Macao, 459-471.

Walling, D.E., 1974. Suspended sediment and solute yields from a small catchments prior to urbanization. In: Gregory, K.J., Walling, D.E. (Eds.). Fluvial processes in instrumented watersheds, *Institute of British geographers special publication*, 6, pp. 169–192.

Walling, D.E., 1978. Suspended sediment and solute response characteristics of the river Exe, Devon, England. In: Davidson-Arnott R., Nickling W. (Eds.), *Research in fluvial systems. Geoabstracts*, Norwich, pp. 169–197.

BIOGRAPHICAL SKETCH

Daniel Mark Stoddard was born in Tacoma, Washington, but moved soon thereafter to Germany where his father served in the United States (U.S.) Army for 2 years. After returning to the U.S., his family relocated to a suburb of Oklahoma City, Oklahoma. The author graduated form Yukon High School and completed his undergraduate degree of B.S. in Mechanical Engineering from Oklahoma State University (OSU).

Upon graduation from OSU, Daniel entered the Navy as a Civil Engineer Corps Officer. His first tour was with Naval Mobile Construction Battalion THREE in Port Hueneme, California where he deployed to Spain and Scotland. His next tour was at the Construction Contracts Office in Norfolk, Virginia, where he administered several multi-million dollar construction and renovation projects at Naval Station Norfolk. His third tour was at SECOND Naval Construction Brigade (2NCB) at Little Creek, Virginia where he was the Eurpoean Projects officer. While at 2NCB, he spent considerable time in Spain, England, Italy, and Greece evaluating various construction projects for the construction battalions.

After completing his Masters Degree in Coastal Engineering, he will proceed to U.S. Navy Dive School in Panama City, Florida and then on to an exciting job in the Naval Ocean Facilities Program.